Performance and Heat Loss of a Coaxial Teflon Pulsed Plasma Thruster[*]

Filip Rysanek and Rodney Burton
University of Illinois Urbana-Champaign
306 Talbot Lab
104 South Wright St.
Urbana, IL 61801
(217) 244-5598
frysanek@uiuc.edu
(217) 244-6223
rburton@uiuc.edu

A coaxial Teflon pulsed plasma thruster, UIUC PPT-7, was tested and results were reported in a previous paper. More thrust data is taken while varying the stored energy for different geometries. A thermal model is used to determine energy lost as heat from the thruster to be 14% of the available energy. A similar thermal model is used to estimate the portion of heat lost due to conduction into the Teflon fuel. The plasma current is curve-fit to reveal a linearly increasing plasma resistance. The plasma temperature is estimated to vary from 9000 K to 21000 K.

Introduction

The pulsed plasma thruster is a robust, solid state device that has flown on a number of missions.[1] The PPT uses a high current, several microsecond pulse to evaporate, ionize, and accelerate a solid fuel to produce thrust. The power input can be throttled by varying either the energy of each pulse, or the pulse rate, making it a versatile thruster capable of performing both attitude control missions as well as orbit raising. Since the fuel is inert and solid, usually Teflon, PPT fuel feed mechanisms are relatively simple, and the fuel itself is safe to handle. PPTs have higher I_{sp} than chemical thrusters, which allows a higher payload mass.

In a previous paper[2] the performance of UIUC PPT-7, an electrothermal, coaxial pulsed plasma thruster was reported. The Two-Stream model was used to describe the thruster efficiency. Since then, more tests have been performed, resulting in a greater understanding of the performance versus energy of the thruster. Also, temperature data is examined to help discuss the heat loss of the thruster.

Experiments

Apparatus
Experiments were performed to help determine the effects of geometry and energy on the performance of an electrothermal thruster. The thruster (Figure 1) is coaxial, with tubular Teflon propellant. The tube is clamped inside a Teflon bracket, which also supports the central brass electrode. A cross-section of the fuel cavity showing the bracket assembly is shown in Figure 2. The front end of the cavity connects to a 17.3 mm long boron nitride nozzle with a 25° half angle. An integral semiconductor type spark plug,[3] used to initiate the discharge, is mounted in the nozzle. The 29 mm diameter cathode is at the exit of the nozzle.

Tests with stored energy less than 50 J use 14 parallel mica capacitor sections,[3] with a total capacitance of 9.2 µF. In order to test at 70 J, 7 more sections are added, increasing the capacitance to 14.1 µF. The 50 J baseline current, shown in Figure 3 is under-damped and displays a peak current of 27 kA at 160 kHz. In order to curve-fit the current data, the resistance has to

---

be estimated. Previously, the resistance has been estimated using the relation:

$$R = \frac{E_{pl}}{\Psi} \text{ [ohms]} \quad (1)$$

where $\Psi = \int I^2 dt$ and E_{pl} is the energy in the plasma. However, when this resistance is used to curve-fit to the experimental data, it becomes apparent that the resistance is not constant throughout the pulse. The plasma current is best fit with a linearly increasing resistance, as shown in Figure 3, increasing from 21 mΩ to 60 mΩ throughout the 13 μs current pulse.

A number of diagnostics were used during these tests. The UIUC compact thrust stand[4] was used in single pulse mode to measure the thrust. At least 10 thrust measurements were taken for each geometry tested. The current was measured using a Rogowski coil on the central electrode. A 1000:1 high voltage probe (Tektronix P6015) was used to measure the capacitor discharge voltage at the vacuum tank feed-through. Temperature measurements of the propellant and one capacitor pack were taken using type K thermocouples. The location of the thermocouples is shown on Figure 2. The mass of the fuel was recorded to within 0.1 mg before and after each 2000 pulse test.

The thruster and capacitor surface temperature measurements were used to determine the heat loss from the thruster and the transfer loss. Starting from room temperature with a constant pulse rate, the capacitor temperature was observed to rise linearly at the outer surface. Assuming that the temperature is uniform throughout the capacitor the power lost to heating is calculated from the measured constant temperature rise rate and the thermal mass (mC_p), according to

$$\dot{Q} = mC_p \dot{T} \quad (2)$$

The thermal mass of the capacitors, listed in Table 1, was determined calorimetricly, using a dewar, by submerging a capacitor section in an equal mass of warm water. The heating of the capacitor due to heat flow through the transmission line from the thruster is estimated as only a small fraction of a watt.

Because the heat from the Teflon cavity is flowing radially through the thruster body, the temperature is not uniform throughout. For this reason, the above equation cannot be used to determine the power lost as heat in the thruster. A heat flow model described later is employed to match the temperature rise rate at the outer surface of the fuel to the power lost to heating.

Table 1 Thermal masses used in heat loss calculations

Item	Mass [g]	mC_p [J/°C]
9.2 μF Capacitor	2390	1780
14.1 μF Capacitor	3520	2630

Tests

Each geometry tested is characterized by the cavity diameter near the rear electrode, the cavity length, and the cavity exit diameter. The baseline constant diameter geometry for these experiments is 14/35/14, denoting a 14 mm rear cavity diameter, 35 mm length, and a 14 mm front cavity diameter. From this baseline case, three other diameters and two other lengths were tested. Tests were also performed without a nozzle in order to determine its effect on performance. Two lengths of tapered cavities were also tested: 3.5/20/14 and 3.5/35/14 with 15° and 10° half angle respectively. These test parameters are illustrated in Table 2. The baseline energy is 50 J, with 5 other energies tested. In order to help illustrate the difference in heat loss at different energies, a test was run at the same power as the baseline, but a different energy, the results of which were reported previously[2].

Table 2 List of parameters varied from baseline

Parameter	Values
Diameter	8,11,14,17 [mm]
Length	20,35,50 [mm]
Energy	10,12.5 J (4 Hz),15,20,28, 50,70 [J]
Pulse Rate	1 Hz, 4 Hz
Taper	10° half angle, 15° half angle
Nozzle	With nozzle, Without Nozzle

Since the previous paper, Tests were performed in order to establish thrust trends versus energy at geometries with a smaller diameter than the baseline. Thrust was measured at different energies on 8/20/8 and 8/35/8 geometries.

Test procedure

Each test consisted of 1000 shots repetitive firing at 1 Hz to warm up the thruster and burn-in the fuel tube. After burn-in, 10 thrust measurements were taken in single pulse mode, followed by another 1000 shots to reduce error in the mass loss measurement. Each pulse produces a thrust stand position transducer (LVDT) output which is a slowly decaying sinusoid.

The initial (t = 0) slope is determined by curve-fitting an analytical damped sinusoid to the LVDT waveform, which gives the post-pulse thrust stand platform velocity u_p. The impulse bit is u_p multiplied by the platform mass, which is weighed for each test setup. Thermocouple data, including the capacitor and fuel temperature, were recorded during all repetitive pulsing phases of the test.

The second set of data, measuring the variation of thrust versus energy at 8 mm diameter, were performed with a slightly different procedure. After the pumps reached operating pressure, the thruster was fired 1000 times at 50 J, 1 Hz to warm up the fuel and thruster. Then, approximately 10 single shot thrust measurements were taken at energies ranging from 50 J to 10 J. If the thruster fired repeatably at lower energies, thrust was also measured at energies below 10 J.

Results

The following plots represent the data taken. Figure 4 - Figure 6 show the specific mass loss, specific thrust, and specific impulse versus energy respectively. Figure 7 - Figure 9 show the same performance parameters plotted versus cavity length. Figure 10 - Figure 12 are plots of the same parameters, but plotted versus cavity diameter. These plots have data points representing the no-nozzle case, and the tapered cavity cases. Figure 13 - Figure 14 representing data taken since the last paper, show the thrust versus energy for the tests with 8 mm diameters.

In order to use this data while designing a PPT, a curve fit was developed for each of the data sets. The specific thrust vs. energy data is curve-fit to:

$$T_{sp} = a - b'/E_o \qquad (3)$$

The specific mass loss (ML) vs energy is then curve-fit using a cubic polynomial fit. The specific impulse vs energy curve fit is then calculated using the specific thrust and specific mass loss fits acording to the equation $I_{sp} = T_{sp}/(g_oML)$. Specific thrust and specific mass loss vs diameter and length is also curve-fit using the above polynomial fit. The corresponding specific impulse curve fit is calculated as above. Some of the polynomial curve fits were determined without consideration of possible data outside the range of the data points. For this reason, extrapolation using these curve fits may be erronious. Table 3 lists the polynomial coefficients and the domain of measured data. Figure 4 - Figure 14 show the curve fits along with the measured data. Table 4

shows the curve fit data for the specific thrust vs stored energy of the 8 mm consant diameter.

Table 3 Curve fit parameters for data around baseline 14/35/14 geometry. $a+bx+cx^2+dx^3$

	ML vs energy	Tsp vs diameter	ML vs diameter	Tsp vs length	ML vs length
a	7.547	46.1	20.3	15.6	1.32
b	0.109	-0.05	-1.42	0.580	0.183
c	-2.7E-3	-0.05	0.040	0	0
d	1.7E-5	0	0	0	0
domain	[10,70]	[8,18]	[8,18]	[20,50]	[20,50]

Table 4 Curve fit parameters for specific thrust vs stored energy for baseline and 8 mm constant diameter data

	14/35/14	8/20/8	8/35/8
a [μN-s/J]	40.3	31.2	44.0
b' [μN-s]	130.4	66.3	213.2
domain [J]	[10,70]	[5,50]	[8,50]

Analysis

The thruster efficiency η_t can be expressed as the product of component sub-efficiencies.[8] These efficiencies include the pulse energy transfer η_{tr}, thruster heat loss η_h, frozen flow η_f, exhaust beam divergence η_{div}, and exhaust velocity distribution efficiency η_{dist}.

$$\eta_t = \eta_{tr} \times \eta_h \times \eta_{ff} \times \eta_{div} \times \eta_{dist} \qquad (4)$$

The transfer efficiency takes into account the energy lost to the equivalent series resistance (ESR) of the capacitor. This energy is estimated from the temperature increase during a 50 W test, and the thermal mass of the capacitor. A small portion of the heating power is due to heat flow from the thruster, however that amount is insignificant compared to the thruster heating. For the baseline case, Q = 2.5 W This is 5.0% of the 50 W making the η_{tr} = 0.95. Another way to estimate the transfer efficiency is from the relation capacitor heating/pulse = $\Psi \times ESR$. A separately-measured capacitor ESR[3] of 2.8 mΩ for the baseline case gives 4.5 W, making η_{tr} = 0.91. We adopt a value of η_{tr} = 0.93. The energy in the Plasma E_{pl} is therefore the stored capacitor energy reduced by capacitor and wall/electrode heat losses, or E_{pl} = $\eta_{tr}\eta_h E_o$.

Mass loss. The pulse specific mass loss (μg/J) is relatively constant with energy for the baseline (14/35/14) geometry. For constant energy (50 J), specific mass loss is seen to increase for decreasing

diameters (Figure 10), presumably because of the higher current density and temperature. The specific mass loss is approximately proportional to length (Figure 7), as reported previously.[5-7]

Specific Thrust. The specific thrust is linear with length at 50 J. It increases monotonically with decreasing diameter, possibly due to lower heat loss with reduced Teflon surface area exposed to the discharge. The specific thrust of the baseline geometry is relatively constant with energy at 35 - 38 μN-s/J from 20 – 70 J, and then decreases significantly (Eq. 3) at lower energies. For the 8 mm constant diameter cases, specific thrust increases slightly with energy from 20 – 50 J. Below 20 J, the specific thrust decreases similarly to the baseline case.

This behavior is consistent with a heat loss model of $\Delta Q_{loss} = B + AE_o$. Assuming that the specific thrust scales as $T_{sp} = C\, E_{pl}/E_o$, it can be shown that:

$$T_{sp}=C(\eta_{tr} - A - B/E_o) \qquad (5)$$

which is mathematically of the same form as the curve fit of Eq. 3. By comparing Eq. 5 to the curve fit Eq. 3, values of the constant can be extracted. For the baseline geometry, the constant C is 46 μN-s/J, A = 0.06, and B = 2.8 J, so that $T_{sp} = 46(0.87 - 2.8/E_o)$ and the heat loss is $\Delta Q_{loss} = 2.8 + 0.06E_o$. At $E_o = 50$ J, $\Delta Q_{loss} = 5.8$ J, approximately 50% from the constant term B and 50% from the term proportional to discharge energy.

We have speculated as to the origin of the constant term of 2.8 J. One possibility is that the plasma pulse quickly raises the Teflon surface temperature to the vaporization point, where it is capped by the sublimation process, freezing the temperature profile and therefore the heat conducted into the solid. This picture suggests that shorter pulse lengths would reduce the constant term in the ΔQ_{loss} equation.

Applying this model to the specific thrust curve fit of Table 4 the heat loss efficiency of the 8 mm diameter geometries is 80 - 90% similar to that of the baseline case.

Specific Impulse. Specific impulse generally increases with energy, from 330 s at 10 J to 490 s at 70 J (baseline geometry). With diameter, I_{sp} reaches a maximum of 450 s at 14 mm (baseline). I_{sp} increases to above 500 s for lengths < 25 mm, and some benefits (610 s) is shown for a short tapered cavity.

Heat loss

In this paper, we are mostly concerned with the heat loss efficiency, the other efficiencies are described elsewhere.[2] The thruster heat loss efficiency is measured from the temperature rise above room temperature for a given time interval. More specifically, the temperature rise rate from room temperature is used along with an analytical model of the radial heat flow through a hollow tube wall of inner radius equal to the fuel cavity radius, and outer radius equal to the radial location of the thermocouple. [Ref. 9 pp 332-333]. The thermal mass of the model does not necessarily correspond to the thermal mass of the thruster, since there are parts of the thruster including the central electrode, nozzle, and back boron nitride insulator, which receive a significant portion of the heat, either directly from the plasma or through conduction. For this reason, the power lost according to the model is scaled by the ratio of the thermal mass of the thruster and that of the model. Since heat distributes itself slowly throughout the entire thruster, only the parts of the thruster in mechanical contact with the arc and fuel were used to determine a thermal mass. Those items and their specific heats are listed in Table 5.

The specific heat of Teflon is unclear, as two reliable sources contain conflicting data. Reference 10 shows the specific heat of Teflon ranging between 0.9 and 1.25 [J/kg-K], while Reference 15 listed values for C_p between 1.2 and 1.5 [J/kg-K]. For this paper, the later values are used.

Table 5 Thruster thermal mass summary

Part	Mass [g]	mC_p [J/°C]	Material
Fuel Tube	26.8	37.5	Teflon
Fuel Clamp 2 ea.	102.0	142.8	Teflon
Fuel Clamp Plates	20.6	18.5	Aluminum
Central Electrode	113.6	42.7	Brass
Standoff 4ea	15.3	7.2	Steel
Standoff Screws	17.4	8.0	Steel
Nozzle	18.0	14.3	
Back Boron Nitride	16.4	13.0	
Total	296	284	

The analytical model used calculates the radial temperature distribution inside of a hollow tube wall of Teflon, subject to boundary conditions at the inner and outer radii of the tube. The model used allows for

a number of possible boundary conditions described by

$$k_1 \frac{\partial T}{\partial r} - k_2 T = k_3 \qquad \text{at } r = r_i \qquad (6a)$$

$$kp_1 \frac{\partial T}{\partial r} - kp_2 T = kp_3 \qquad \text{at } r = r_o \qquad (6b)$$

where T is the temperature, r is the radius, r_i is the inner radius, r_o is the outer radius, and k_1, k_2, k_3, kp_1, kp_2, kp_3, are all constants. The model begins with temperature of 0° everywhere. Since all the calculations are based on temperature differences, starting from room temperature does not affect the outcome.

The boundary conditions required involve a constant influx of energy at the inner radius, and zero efflux of energy at the outer radius. Due to a numerical problem, it is not possible to make both the inner and outer radius boundary conditions contain only derivative terms with k_3 or kp_3 equal to zero, so a small temperature dependence is added to the efflux of energy at the outer radius. The empirically determined constants for the baseline case are listed in Table 6. Since the outer temperature change in the experiment never reached 20 degrees, the efflux of energy in the model is negligible.

Table 6 Constants used in heat transfer model boundary condition

Constant	k_1	k_2	k_3	kp_1	kp_2	kp_3
Value	1	0	6600	10	1	1

For this conductive thermal model the constant k_3 determines the amount of power influx into the hollow tube at the inner radius. The power influx can be calculated using the equation

$$\dot{Q} = kA \frac{\partial T}{\partial r} \qquad (7)$$

where k is the solid Teflon thermal conductivity, A is the surface area of the inside of the tube, and $\partial T / \partial r = k_3$. Figure 15 shows the experimental temperature rise for each 1000 pulse sequence, along with the model results for the baseline case. From the model, 2.4 Watts of power was lost as heating. However, the thermal mass used in the model is 106 J/°C, so a correction factor of 284/106 is used resulting in a power lost to heating of 6.4 W. This is 13.8% of the 46.5 Watts left from the capacitors, making $\eta_h = 0.86$

Table 7 Heat loss summary

	Power [Watts]	Efficiency
Power in	50	
Capacitor	3.5±1.0	$\eta_{tr} = 0.93$
Thruster	6.4	$\eta_h = 0.86$

The energy in the plasma is then $E_{pl} = (\eta_{tr}\eta_h)E_o = (0.80) E_o$, or 40 J for the baseline case.

Surface Heat Conduction
From the above model, it was determined that 6.4 Joules of energy is lost to thruster heating for every 50 J pulse. A portion of that heat is deposited into the electrode through sheath losses. The rest is deposited into the Teflon. As energy is deposited into the Teflon fuel, three processes are occurring. Heat is conducted into the fuel, heat is radiated out of the fuel, and heat is lost when fuel evaporates. This paper considers the convection of heat into the solid Teflon from the high temperature plasma. The time-dependent temperature distribution inside the Teflon immediately after one pulse is obtained by using a model similar to the one used in the heat transfer analysis, with constant initial temperature throughout the Teflon except at the surface, according to the following equation. [Ref 9 pp 205-208].

$$-\pi \sum G(v_1, v_2, a, b, \alpha_n) e^{-\kappa \alpha_n^2 t} + \\ + \frac{v_1 \ln(b/r) + v_2 \ln(r/a)}{\ln(b/a)} \qquad (8)$$

where $G(v_1, v_2, a, b, \alpha_n)$ is

$$\frac{[\{v_2 J_0(a\alpha_n) - v_1 J_0(b\alpha_n)\} J_0(a\alpha_n) U_0(r\alpha_n)]}{J_0^2(a\alpha_n) - J_0^2(b\alpha_n)}$$

the constants a and b are the inner and outer radius of the Teflon fuel, v_1 and v_2 are the surface temperatures at the inner and outer surface respectively. α_n is the nth root of

$$J_0(\alpha a)Y_0(\alpha b) - J_0(\alpha b)Y_0(\alpha a) = 0 \qquad (9)$$

where J_0 and Y_0 are Bessel functions. U_0 is the relation

$$J_0(\alpha r)Y_0(\alpha b) - J_0(\alpha b)Y_0(\alpha r) \qquad (10)$$

and κ is the diffusivity which is $K/\rho C_p$ or 7.8×10^{-8} for Teflon.

The model requires knowing the surface temperature of the Teflon. It is assumed that the pressure in the cavity is the same as the vapor pressure of the Teflon. The vapor pressure of Teflon follows the equation:

$$p_{vap} = p_c \exp(-T_c / T_s) \qquad (11)$$

where $p_c = 1.84 \times 10^{15}$ and $T_c = 20800$ K. Eq. 11 is a curve fit of data from reference 10, using the Clausius-Clapeyron equation to fit the data.[1] The fit and data are shown in Figure 16. The cavity pressure is estimated using the equation $p=(\gamma-1)E_{pl}/V$ where γ is the ratio of the specific heats and V is the cavity volume. The ratio of specific heats γ is determined as 1.074 from thermodynamic data for Teflon[11] at 20000 K. This results in $p \approx 5$ atm (5×10^5 Pa) for the baseline geometry at 50 J. From Figure 16, this corresponds to a surface temperature of 675°C required to generate $p_{vap} = 5$ atm.

To estimate the length of time that the Teflon surface temperature remains at 675°C the sonic velocity of the plasma during the current pulse is determined by estimating plasma temperature. The plasma resistance, determined by subtracting the ESR from the circuit resistance used to curve-fit the current data (Figure 3), is then correlated to the plasma temperature using the Spitzer resistivity assuming the electron-neutral collision frequency is much smaller than electron-ion ($\nu_{eo} << \nu_{ei}$):[12]

$$R = \eta \frac{L}{\pi/4 \, D^2} = .0067 \left(\frac{L}{r^2} \right) \left(\frac{1}{T_{ev}^{3/2}} \right) Z \ln \Lambda \text{ [ohms] (12)}$$

$\ln\Lambda$ is determined according to:

$$\ln \Lambda = 23.4 - 1.15 \, Log(n_e) + 3.45 \, Log(T_{ev}) \qquad (13)$$

The electron density n_e (in cm^{-3}) needed for $\ln\Lambda$ is determined using the Saha equation for a gas mixture, assuming only single ionization[13]:

$$K_C(T) = \frac{n_{C^+} n_e}{n_C} = \frac{2(2\pi m_e kT)^{3/2}}{h^3} \left(\frac{f_C^{i+}}{f_C^i} \right) e^{\left(-\varepsilon_c / kT \right)} \quad (14a)$$

$$K_F(T) = \frac{n_{F^+} n_e}{n_F} = \frac{2(2\pi m_e kT)^{3/2}}{h^3} \left(\frac{f_F^{i+}}{f_F^i} \right) e^{\left(-\varepsilon_f / kT \right)} \quad (14b)$$

The partition function ratios are found from spectral data[14] and are 0.53 for carbon and 1.68 for fluorine.

The following equations are then used to solve for the electron density n_e

$$p = (n_e + n_C + n_C^+ + n_F + n_F^+)kT \qquad (15)$$

$$n_e = n_C^+ + n_F^+ = \frac{n_C^0 K_C}{n_e + K_C} + \frac{n_F^0 K_F}{n_e + K_F} \qquad (16)$$

Figure 17 shows a plot of the resistance versus plasma temperature at 1, 5, and 10 atm. From this analysis, the plasma temperature ranges from 21000 K at the beginning of the pulse, to 9000 K at the end. From Ref. 11 these temps correspond to a sonic velocity ranging from 5000 to 2500 m/s.

A rough estimate of conductive and radiative heating rate of the Teflon surface exposed to this temperature plasma at several atm predicts that the temperature rises to 675°C in a short time compared to the pulse length. Using the sonic velocity determined above, the length of time it would take an expansion wave to travel from the cavity entrance to the rear electrode is approximately 8 μs. For this model, since parts of the Teflon surface would be cooled before the expansion wave would reach the end of the cavity, it is assumed that the Teflon surface no longer absorbs heat from the plasma 4 μs after the current pulse.

The measured heat loss of 6.4 J/pulse can be accounted for from two sources: a) heat stored in a thin surface layer of Teflon, and b) heat transferred to the electrodes by the voltage sheaths during the pulse. By using the thermal conduction model, a temperature distribution extending approximately 5 μm inside the Teflon is developed at the end of the pulse. From Ref 10 the specific heat of Teflon includes a phase change from crystalline to amorphous, corresponding to 59 J/g at 600 K. Using a constant C_p of 1.4 J/kg-K the temperature distribution corresponds to 4.2 Joules of energy stored in the Teflon in the form of heat. This value is increased by 10% to account for the phase change to a final value of 4.6 Joules. This accounts for 72% of the energy lost due to thruster heating. The remaining heat (1.8 J) can be accounted for by the sheath loss at the electrodes, assuming ~20 V total drop.

Conclusions

The specific thrust vs energy for geometries with a smaller diameter cavity than the baseline show a specific Thrust variation of $T_{sp}=a-b'/E_o$, similar to the baseline case. A thermal model was used to show the

transfer efficiency η_{tr}=0.93 and the heat loss efficiency η_h = 0.86, corresponding to 6.4 J lost to the wall out of 50 J stored. The plasma current was curve-fit to reveal a linearly increasing plasma resistance from which the plasma temperature is estimated to vary from 9000 K to 21000 K. A thermal model is used to estimate that 72% of heat lost is by convection into the Teflon fuel and the remainder is due to the sheath drop.

Acknowledgements

References

1. R. L. Burton, P. J. Turchi, "Pulsed Plasma Thruster," *Journal of Propulsion and Power*, Vol. 14, No. 5, 1998, pp. 716-735.
2. Rysanek, F., Burton, R. L., "Effects of Geometry and Energy on a Coaxial Teflon Pulsed Plasma Thruster" AIAA Paper No. 2000-3429, July, 2000.
3. Unison Industries, Jacksonville, FL 32256
4. Wilson, M. J., Bushman, S. S., and Burton, R. L., "A Compact Thrust Stand for Pulsed Plasma Thrusters," IEPC Paper No. 97-122, 25th International Electric Propulsion Conference, Cleveland, OH, Aug., 1997.
5. Bushman, S. S., Burton, R. L., and Antonsen, E. L., "Arc Measurements and Performance Characteristics of a Coaxial Pulsed Plasma Thruster," AIAA Paper No. 98-3660, July, 1998.
6. Bushman, S. S., "Investigations of a Coaxial Pulsed Plasma Thruster," University of Illinois M.S. Thesis, University of Illinois College of Engineering Rpt. No. UILU-ENG 99-0509, AAE Report 99-09, 1999.
7. Keidar, M., "Electrical Discharge in the Teflon Cavity of a Coaxial Pulsed Plasma Thruster," IEEE Transactions on Plasma Science, Vol. 28, No. 2, Apr. 2000.
8. Burton, R. L., Rysanek, F., Antonsen, E. A., Wilson, M. J., and Bushman, S. S., "Pulsed Plasma Thruster Performance for Microspacecraft Propulsion," Chap. 13, AIAA Progress Series, Micropropulsion for Small Spacecraft, M. Micci, ed., 2000.
9. Carslaw, H. S., and Jaeger J. C., Conduction of Heat in Solids, 2nd Ed., Oxford University Press, 1959.
10. Wentink, T., Jr., "High Temperature Behavior of Teflon," AVCO-Everett Research Laboratory, AF04(647)-278, Everett, MA, July 1959.
11. Kovitya, P., "Thermodynamic and Transport Properties of Ablated Vapors of PTFE, Alumina, Perspex, and PVC in the Temperature Range 5000 - 30,000 K," IEEE Transactions on Plasma Science, Vol. PS-12, No. 1, March 1984, pp 38 – 42.
12. Spitzer, L., Physics of Fully Ionized Gases, 2nd Ed., Interscience Publishers, 1962.
13. Jahn, R. G., Physics of Electric Propulsion, McGraw-Hill Book Co., New York, NY, 1968
14. http://physlab2.nist.gov/cgi-bin/AtData/levels_form
15. Dr. Bro. Dupont. Private conversation.

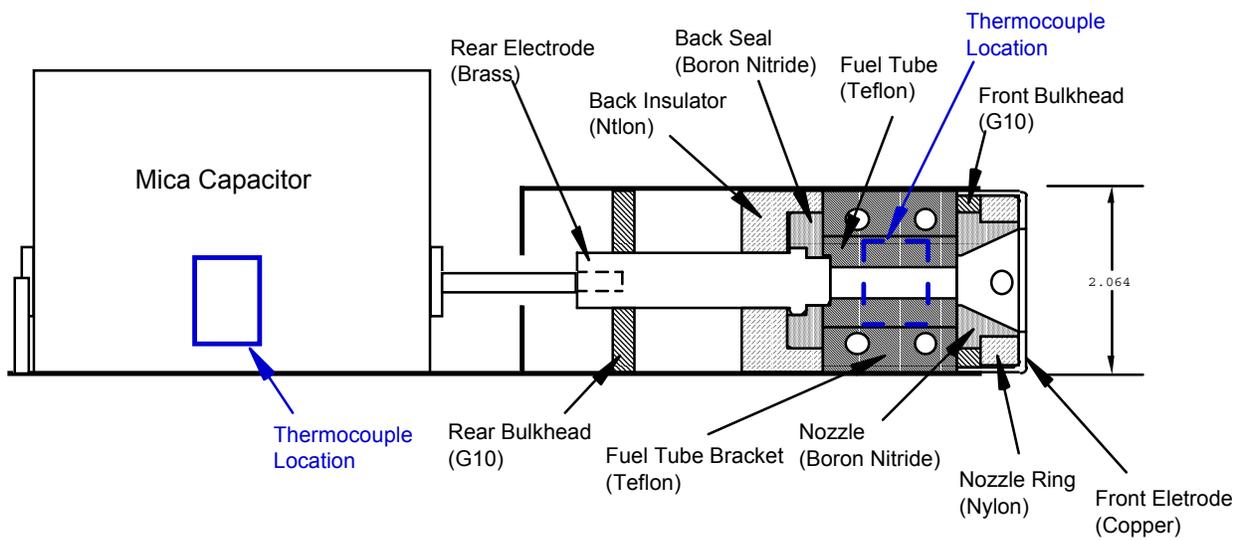Figure 1 PPT-7 Coaxial electrothermal pulsed plasma thruster

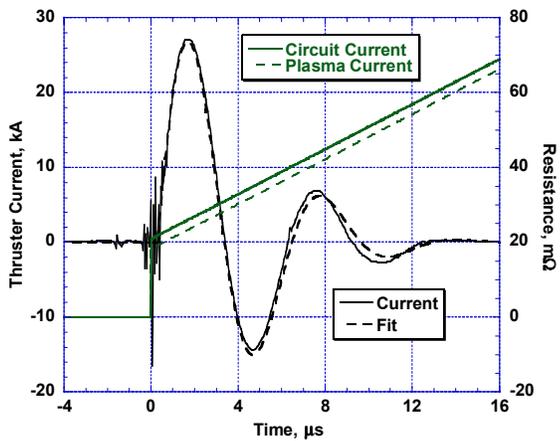Figure 2 - Cross-sectional schematic of PPT-7

Figure 3 - Baseline pulse current with curve fit based on linearly increasing resistance
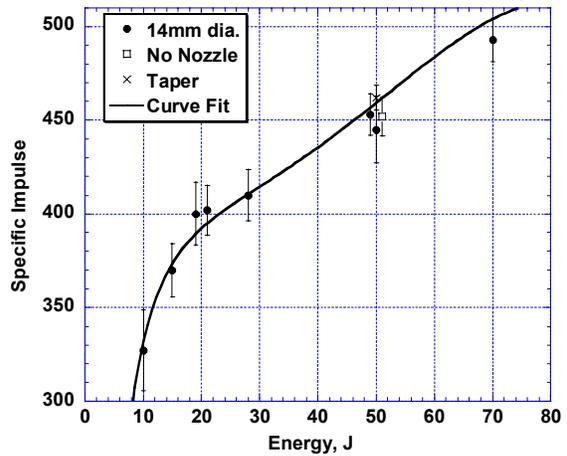

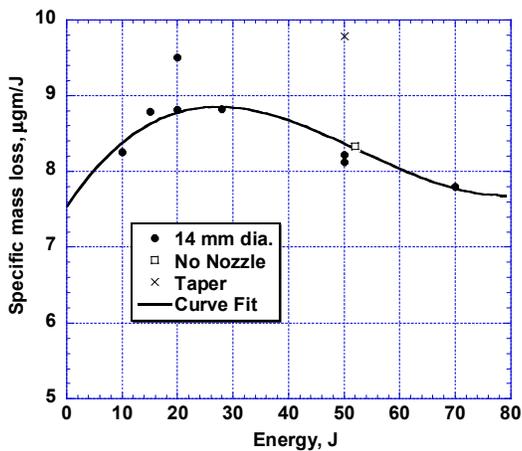Figure 6 – Specific impulse vs energy for baseline 14/35/14 case

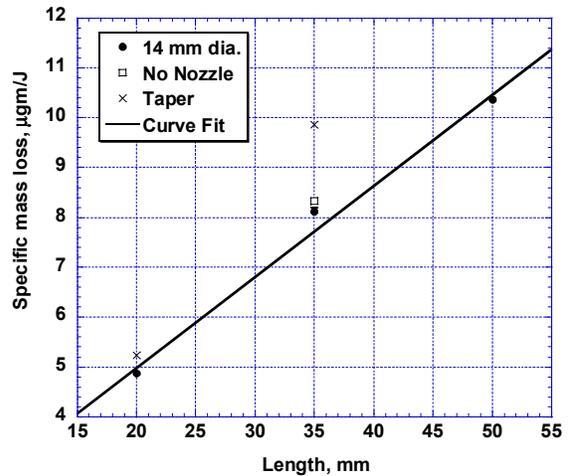Figure 4 - Specific mass loss vs energy for baseline 14/35/14 case.

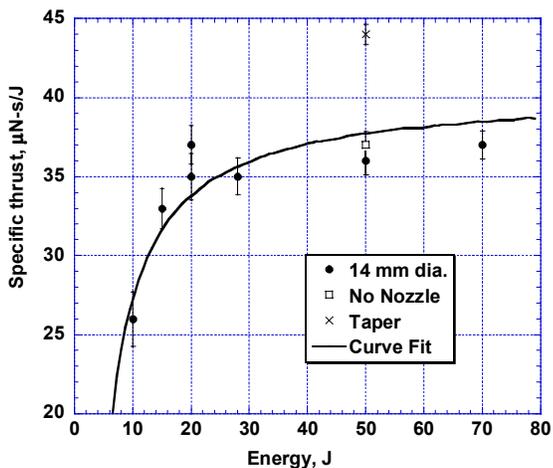Figure 7 – Specific mass loss vs cavity length at E_o = 50 J.

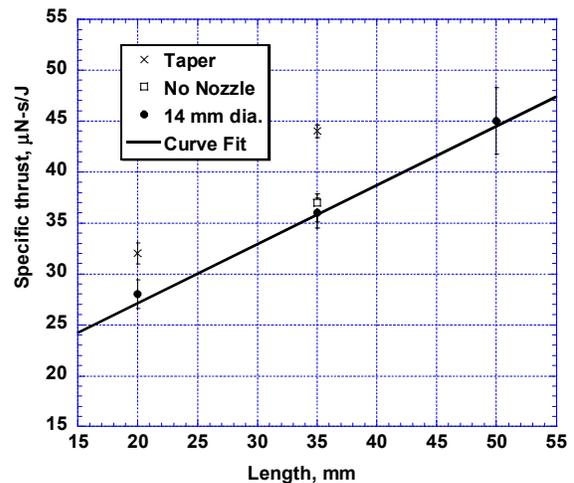Figure 5 – Specific thrust vs energy for baseline 14/35/14 case

Figure 8 – Specific thrust vs cavity length at E_o = 50 J.
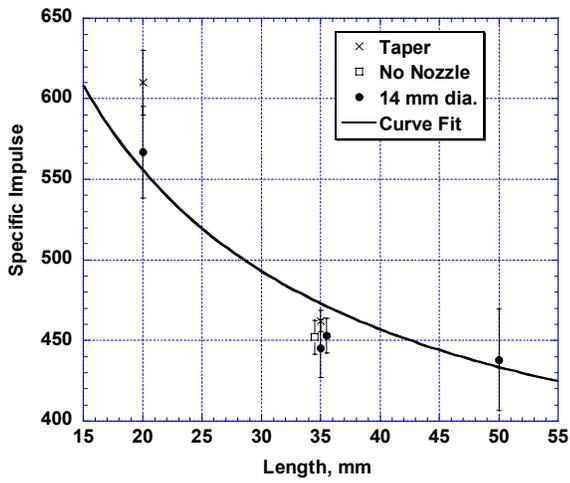
Figure 9 – Specific impulse vs cavity length at E_O = 50 J
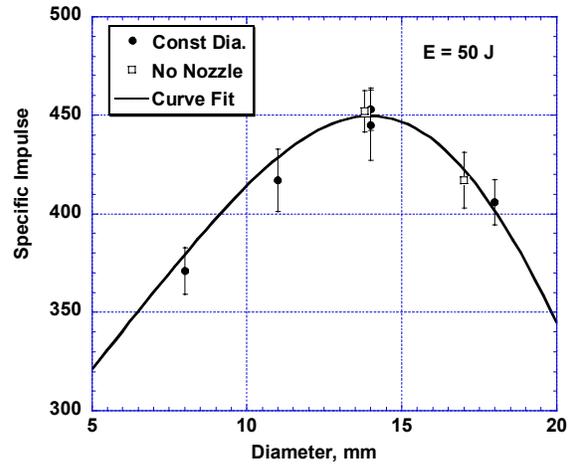
Figure 12 – Specific impulse vs cavity diameter at E_O = 50 J
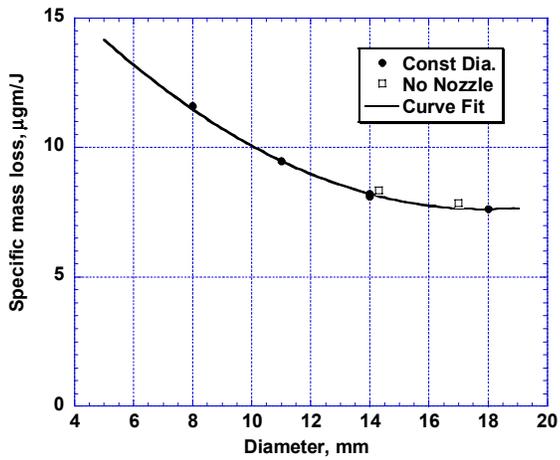
Figure 10 – Specific mass loss vs cavity diameter at E_O = 50 J
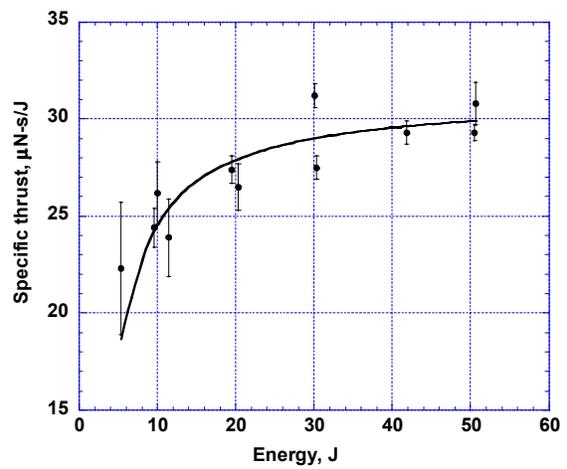
Figure 13 – Specific thrust vs energy for 8/20/8 geometry
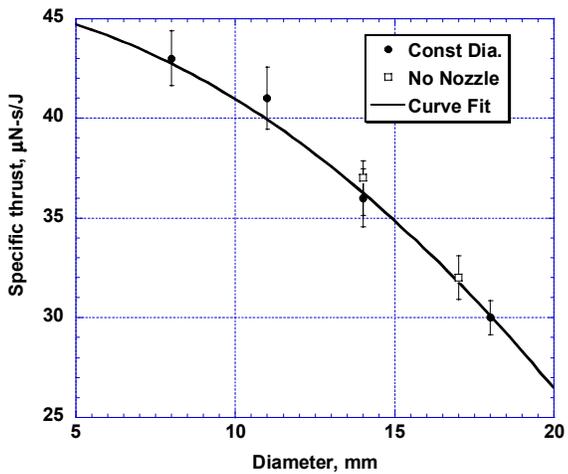
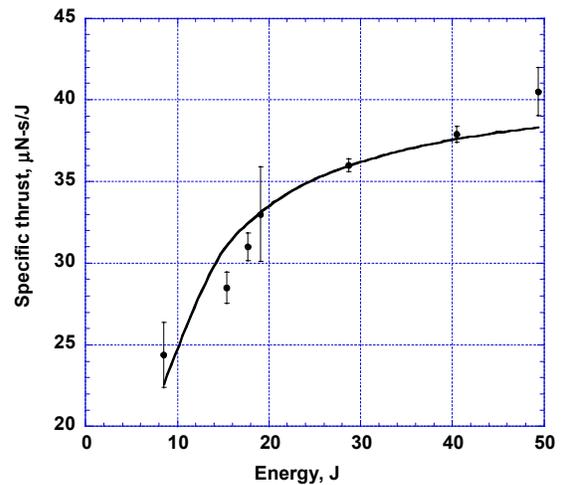Figure 11 – Specific thrust vs cavity diameter at E_O = 50 J

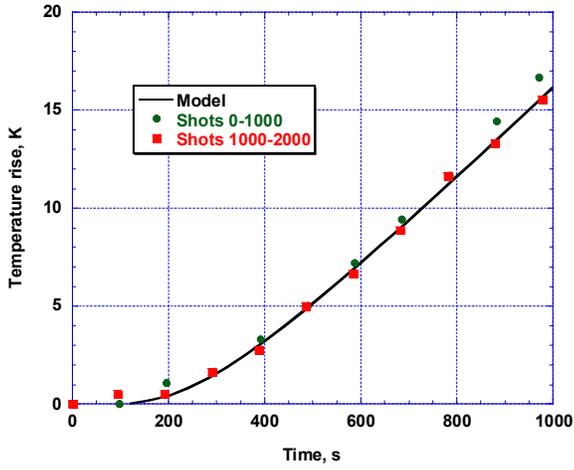Figure 14 – Specific thrust vs energy for 8/35/8 geometry

10

Figure 15 - Temperature rise of thruster during each 1000 pulse sequence for the baseline case with model fit
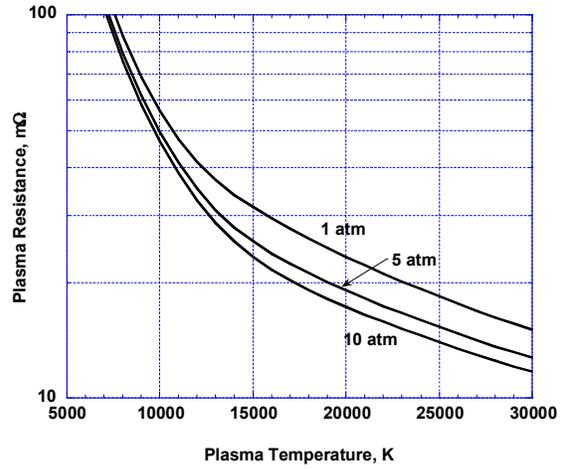

Figure 17 – Plasma resistance vs temperature for PPT-7 Baseline case, calculated at 1, 5, and 10 atm. Measured plasma resistance is 17 – 57 mΩ, allowing plasma temperature to be determined
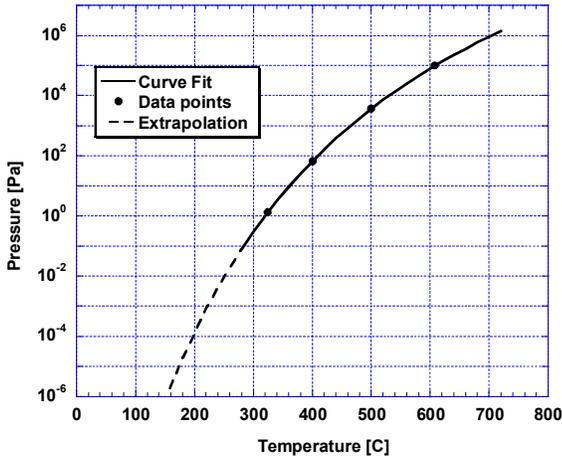

Figure 16 – Vapor pressure of Teflon. Vapor pressure of 1 and 10 atm occur at 600 and 700 °C respectively